In *Proceedings of the 2008 Symposium on Eye Tracking Research and Applications* (ETRA), ACM, New York, pp. 35-38.

Measurement of eye velocity using active illumination

Jeffrey B. Mulligan*
NASA Ames Research Center

Abstract

With speeds measured in hundreds of degrees per second, measurement of saccadic velocities can be a challenging problem, usually solved by the application of high-frame-rate cameras or high-bandwidth analog systems. This paper describes a novel approach utilizing a standard NTSC video camera coupled with an array of near-infrared light-emitting diodes that are flashed at various times within a single frame. The principle has been demonstrated with a prototype apparatus consisting of 4 16-cell linear arrays (”light sticks”). The cells of each light stick are energized sequentially during each video field, while a camera captures their images reflected in the cornea. When the eye is still, the four line segments are aligned with the vertical and horizontal directions, but when the eye is in motion they appear tilted. Opposite light sticks are cycled in opposite directions, producing opposite tilts. Thus, the measurement of velocity is transformed to a measurement of the angle between two line segments. Preliminary results from a prototype system show a noise level of approximately 20 deg/sec.

Keywords: saccadic velocity, saccades, active illumination

1 Introduction

Saccadic eye movements are perhaps the fastest of all movements the human body is capable of, with speeds as high as 500 degrees/second, and durations of some tens of milliseconds. Because of these brief durations, conventional video equipment is generally too slow to capture the fine details of acceleration, flight and braking. Instead, saccades result in blurred images. Several commercial eye-tracker vendors now offer high-speed video-based systems offering frame rates in excess of 1000 Hz, which are capable of measuring saccadic trajectories. The gold standard for this sort of measurement is probably the magnetic search coil technique [Robinson 1963], which has very low noise level and excellent temporal bandwidth, typically sampled at 1000 Hz.

This paper presents a novel approach to the measurement of saccadic velocity using a video camera with a standard frame rate of 60 Hz (after deinterlacing). Instead of one or two compact illumination sources, we use a collection of 4 linear arrays. These arrays are reflected by the front surface of the cornea, and appear as small, bright line segments against the dark background of the pupil. Control circuitry causes each illumination cell to be energized for a brief period of around 1 millisecond, with the cells in each linear array energized sequentially. Our prototype system consists of 4 arrays, two horizontal and two vertical, arranged about a cathode ray tube (CRT) display monitor, as shown in figure 1. Consider what happens when the eye is in flight during the acquisition of a image: because the lights in the illuminator array are lit at different times,

*e-mail: jeffrey.b.mulligan@nasa.gov

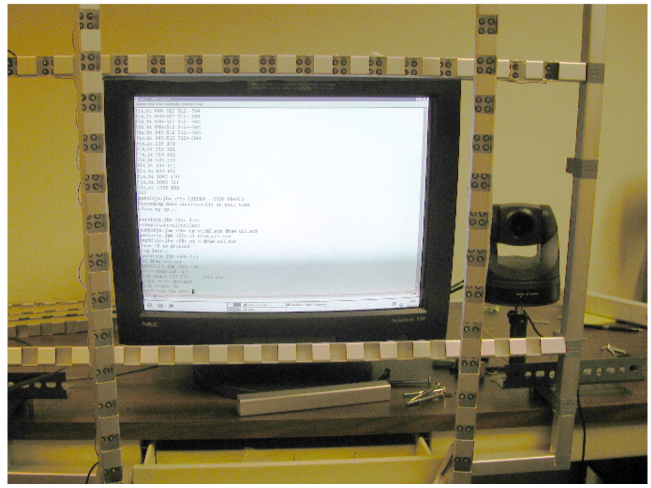

Figure 1: View of the experimental apparatus from the subject's station. LED illuminators are mounted in lengths of square aluminum tubing, configured to surround a large CRT display. A pan-tilt-zoom camera located to the right of the CRT captures images of the eye region of the subject's face.

their reflections will be captured at different positions along the eye's trajectory, and the reflected lines which are normally aligned will appear tilted. Images of the vertical illuminator arrays will be tilted by horizontal motions, vertical motions will produce tilts in the images of the horizontal arrays, and oblique motions affect both. To provide robustness with respect to the relative alignment of the camera with the illuminator arrays, we have arranged for the arrays on opposite sides of the monitor to be cycled in opposite directions; for example, the left vertical array is sequenced top-to-bottom, while the right array is sequenced bottom-to-top. Because of this direction difference, opposite apparent tilts will be induced when the eye moves relative to the camera, and the difference between the two tilts will be invariant under small rotations of the camera about the line-of-sight. Thus, we can estimate the eye velocity by measuring the orientations of 4 line segments in a static image. The remainder of this paper is devoted to a description of the apparatus and associated processing steps, and a small amount of preliminary data.

2 Methods

The heart of the method is the active illumination system, composed of four linear arrays of 16 illumination cells each, and the associated drive and control electronics. A microcontroller (Microchip PIC-16F876) is interfaced to four light-emitting diode (LED) controller chips (Texas Instruments TLC5921), and communicates with the host computer over an RS232 serial interface. The microcontroller also has access to video sync pulses, enabling programs to synchronize execution with the camera. Programs for the microcontroller are written in assembly language, and assembled using GNU PIC utilities (http://gputils.sourceforge.net). The host computer is a dual-processor pentium system running the CentOS distribution of the Linux operating system.

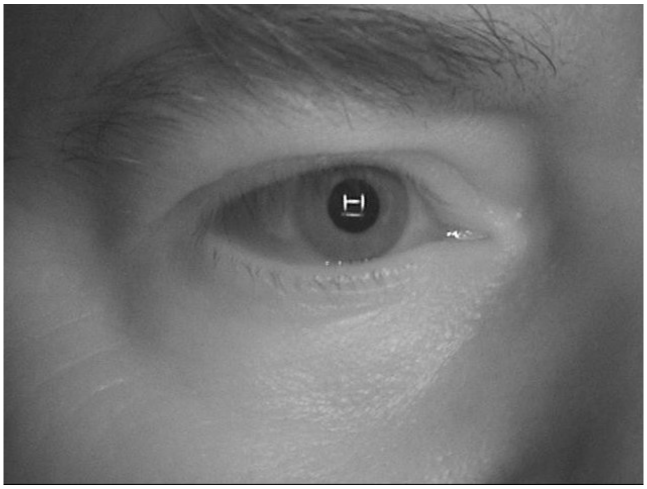

Figure 2: Typical video image obtained during steady fixation. The reflection of the illuminator array can be seen in the pupil.

Each illumination ”cell” is composed of four near-infrared LED’s wired in series. The arrays are fabricated from 1 inch square aluminum tubing, with windows milled out on the front, and holes drilled in the back to accept LED mounting grommets. The depth of the cut-out for the windows is slightly deeper than the thickness of the tubing (1/16”) to facilitate easy installation of plastic holographic ”light-shaping” diffusers (Physical Optics Corporation). The diffusion angle, combined with the angular distribution of the emitted light, determines the volume of space which each light cell illuminates, which by definition is the volume of space in which the corresponding cell will be visible in the image reflected by the cornea.

Four of these ”light sticks” were arrayed around a cathode ray tube (CRT) display monitor. Figure 1 shows the view seen from the subject’s station. The plastic connectors (Brunner Enterprises, West Seneca NY) used to assemble the light sticks were modified by attaching short lengths of 7/8” diameter cylindrical plastic rods; these rods were inserted into the ends of the light sticks, allowing the light sticks to be rotated about their long axis, so as to aim the light at the subjects’ station. The entire assembly was clamped to the table in front of the display monitor.

To verify the safety of the system, the optical power incident at the eye was measured using a thermopile detector (Ophir Optronics, Logan UT) having a spectrally flat response. Application of the ANSI Z136.1-2000 standard [Delori et al. 2007] revealed that the system exposure levels are more than two orders of magnitude below the maximum permissible levels.

Images were acquired using a pan-tilt-zoom camera (Sony EVI-D70), fitted with an infrared filter (B+W #093, equivalent to Wratten 87C). A typical image is shown in figure 2. A second dual-processor microcomputer hosted the frame-grabber (Matrox Meteor-RGB), with a resolution of 640x480. The results described here were all derived from off-line processing of recorded sequences.

Recordings were made while subjects maintained fixation on a small cross displayed on the CRT monitor. A sequence of fixation point locations was presented, with a dwell time of 2 seconds in each location. The target first stepped through a 3x3 calibration grid, then made a series of jumps back and forth along the horizontal midline, with 3 repeats at each of 7 jump sizes. This was then repeated for vertical jumps, and for jumps along both diagonals. Finally, the calibration grid was presented a final time. A total of 186 locations were presented, requiring 6 minutes and 12 seconds for the entire sequence.

The pattern formed by the reflections of our illuminator arrays is quite distinctive and relatively easy to locate. We therefore begin by localizing this feature, and selecting the subimage from the large image which approximately centers it. After deinterlacing and down-sampling by a factor of 2 horizontally (to preserve proper aspect ratio), subsequent processing is restricted to a 32 by 32 region of interest. We register the image to a reference template by applying subpixel shifts, effectively stabilizing the pattern of reflections. (Fortunately, good registration is obtained even when the appearance is distorted.) The pupil margin is localized, providing us with a measure proportional to eye rotation. Finally, the reflection component is isolated, and fit with a model of the light stick appearance, resulting in estimates of the angles of each of the four sticks. A series of glint-stabilized subimages captured during saccades is shown in figure 3.

Calibration of the system consists of separate components: the relation between relative pupil position and gaze direction, and the relation between reflection orientations and eye velocity. For the moderate eye excursions encountered in our dataset, the relationship between relative pupil position and gaze direction is linear. We assume alignment between the display and camera coordinate systems, and therefore do not consider any cross-terms. There are thus a total of four parameters: gain and offset for horizontal and vertical. We assume that the subjects fixated all the targets with reasonable accuracy, and adjusted the calibration parameters to match the data to the stimulus trace. The results allow us to convert the position of the pupil relative to the reflection pattern to a location on the screen.

Velocity calibration was performed using smooth pursuit eye movements of known velocity. Ten cycles of 1 Hz circular motion requiring pursuit at 50 degrees per second were presented while the subject attempted to maintain fixation on the target. The recording was analyzed as described above, and sinusoids were fit to the reflection orientation traces (assuming perfect smooth tracking). The amplitude of the best-fitting sinusoid was used to determine the factor relating degrees of line rotation to eye velocity in degrees per second - typical values ranged between 10 and 20.

3 Results

Figure 4 shows a plot of the pupil position and glint orientation from a six minute recording. The Y axes are labeled in raw camera image units on the left, and in terms of visual angle on the right.

Saccade intervals were localized by aligning the position trace with the (unsynchronized) stimulus trace, allowing us to use the stimulus trace to identify the saccade time, up to the variability in saccadic latency. We then estimated the value of the peak saccadic velocity for a given saccade by simply looking for the maximum magnitude of the angle measurement within a small window centered at the expected time. Representative results for horizontal saccades from one subject are plotted in figure 5, where peak saccadic velocity is plotted as a function of saccade size, tracing out the ”main sequence” [Bahill and Stark 1979; Harwood et al. 1999].

Because the saccades were relatively infrequent in the recordings, the bulk of the measurements were clustered around the values corresponding to zero velocity. We therefore felt justified in estimating the noise level of the system by simply computing the mean and standard deviations of the horizontal and vertical reflection orientations. For the ”best” subject (largest pupils and fewest blinks, and the cleanest data without additional tweaking), the angular standard

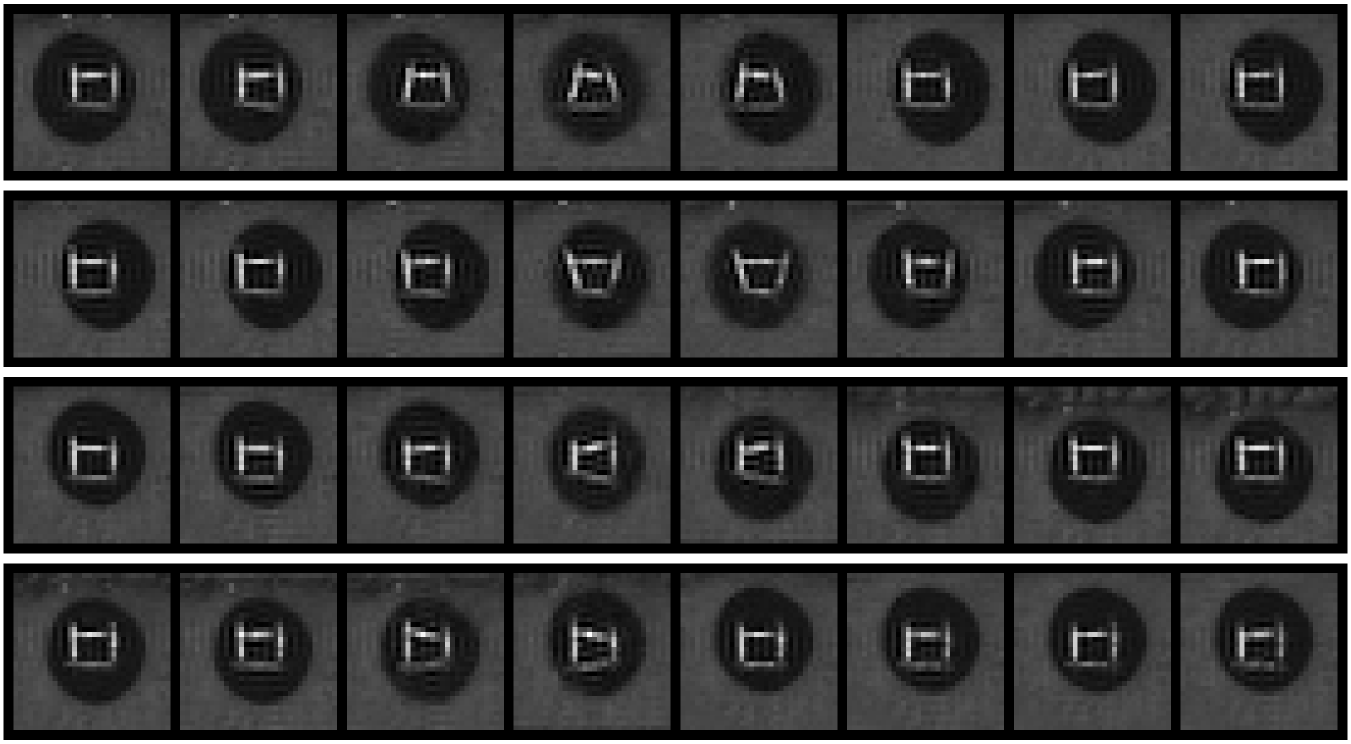

Figure 3: Four 8-frame sequences showing saccades in different directions. First row: leftward saccade (pupil moves right in image), verticals tilted in at top (”A”). Second row: rightward saccade (pupil moves left in image), verticals tilted in at bottom (”V”). Third row: downward saccade, horizontals pinched at left (”left arrow”). Fourth row: upward saccade, horizontals pinched at right (”right arrow”).

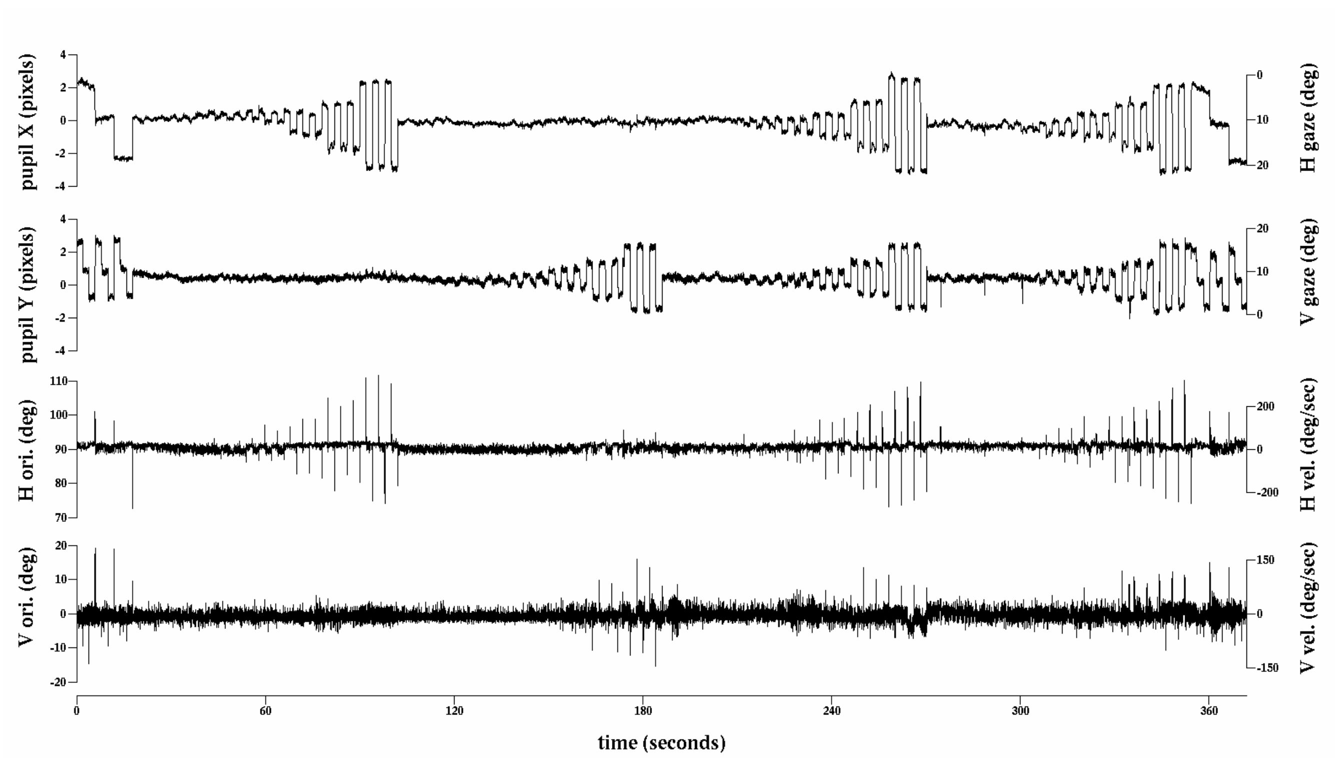

Figure 4: Computed traces showing pupil position (in glint-stabilized images), and saccadic velocity (computed from glint orientations) over the entire 6 minute recording period (subject JBM).

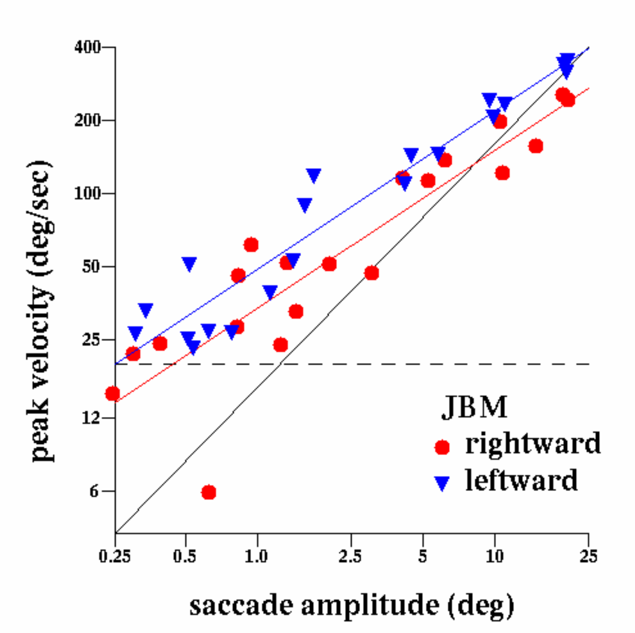

Figure 5: Plot of peak saccadic velocity (measured in single still frames) as a function of saccadic amplitude. The regular relationship observed between these two variables is often referred to as the "main sequence." Subject JBM; inverted triangles are for rightward saccades, while disks are for leftward saccades. The diagonal represents a slope of 1; regression lines are also drawn for the two datasets, with slopes 0.650 (leftward) and 0.646 (rightward). The dashed line indicates the noise floor when the eye is nominally stationary.

deviations were 1.2 degrees for the vertical segments (corresponding to 20 degrees/second of eye movement), and 1.7 degrees for the horizontal segments (corresponding to 16 degrees/second of eye movement).

4 Discussion

The results shown in figure 5 are somewhat noisy, but we are optimistic that better results can be obtained simply by moving the camera closer to the subject. The present arrangement had the advantage that, because the angle subtended between the camera and the illumination system was relatively small, the reflections fell within the pupil for the most part. Moving the subject closer to the apparatus will move the reflection away from the center of the pupil, possibly complicating the processing.

A curious feature seen in figure 5 is the fact that the leftward saccades appear to have slightly higher peak velocities than their rightward brethren. There are several possible explanations. First, it might be the result of some sort of artifact or bias in the angle measurements, resulting from asymmetries in the pattern of the reflections. This is best tested by simply repeating the experiment with a better measurement system. Alternatively, it may instead be a behavioral feature, evincing some facet of the underlying neurophysiology. Left-right asymmetries have been reported for saccadic latencies [Honda 2002], which may reflect a high-level attentional preference for one of the visual hemifields, while asymmetries are also observed in subcortical structures [Sylvester et al. 2007], which are more often nasal-temporal asymmetries rather than left-right asymmetries. These possibilities can be distinguished by testing both eyes.

Although the subjects' heads were stabilized with a chinrest in the current study, our long-term goal is to adapt the system for use with freely-moving subjects. In this case, it will be necessary to use the camera's pan-tilt mechanism to keep the eye region centered in the frame. This task will be aided by our active illumination system: because we obtain velocity information in each frame, we can potentially generate more accurate predictions of the eye's future position. Because the system measures relative motion between the eye and camera, head movements can be tracked in the same way as saccades. (Unfortunately, vibrations of the camera platform also can introduce significant relative motions!) The use of a spatially-structured illuminator produced the serendipitous result that the reflection could be easily located by cross-correlation with template; we expect that this will also be useful in the development of a real-time tracker.

5 Conclusion

We have presented an active illumination system allowing measurement of eye velocity in still images. Using relatively low-resolution images, the system has a noise level of approximately 20 degrees/second. While not yet in the same league as other more precise measurement technologies, the method can be used with relatively inexpensive standard video cameras.

Acknowledgments

Supported by the Integrated Intelligent Flight Deck Technologies (IIFDT) project of NASA's Aviation Safety program.

References

BAHILL, A. T., AND STARK, L. 1979. The trajectories of saccadic eye movements. *Scientific American 240*, 108–117.

DELORI, F. C., WEBB, R. H., AND SLINEY, D. H. 2007. Maximum permissable exposures for ocular safety (ansi 2000), with emphasis on ophthalmic devices. *J. Opt. Soc. Am. A 24*, 1250–1265.

HARWOOD, M. R., MEZEY, L. E., AND HARRIS, C. M. 1999. The spectral main sequence of human saccades. *J. Neuroscience 19(20)*, 9098–9106.

HONDA, H. 2002. Idiosyncratic left-right asymmetries of saccadic latencies: examination in a gap paradigm. *Vision Res. 42*, 1437–1445.

ROBINSON, D. A. 1963. A method of measuring eye movements using a scleral search coil in a magnetic field. *IEEE Trans. Biomed. Eng. 10*, 137–145.

SYLVESTER, R., JOSEPHS, O., DRIVER, J., AND REES, G. 2007. Visual fmri responses in human superior colliculus show a temporal-nasal asymmetry that is absent in lateral geniculate and visual cortex. *J. Neurophys. 97*, 1495–1502.